Magneto-Oscillations due to Electron-Electron Interactions in the ac Conductivity of a Two-Dimensional Electron Gas

T. A. Sedrakyan and M. E. Raikh

Department of Physics, University of Utah, Salt Lake City, Utah 84112, USA

(Received 30 May 2007; published 29 February 2008)

Electron-electron interactions give rise to the correction, $\delta\sigma^{\rm int}(\omega)$, to the ac magnetoconductivity, $\sigma(\omega)$, of a clean 2D electron gas that is periodic in ω_c^{-1}, where ω_c is the cyclotron frequency. Unlike conventional harmonics of the cyclotron resonance, which are periodic with ω, this correction is periodic with $\omega^{3/2}$. Oscillations in $\delta\sigma^{\rm int}(\omega)$ develop at low magnetic fields, $\omega_c \ll \omega$, when the conventional harmonics are suppressed by the disorder. Their origin is a *double* backscattering of an electron from the impurity-induced Friedel oscillations. During the time $\sim\omega^{-1}$ between the two backscattering events the electron travels only a *small portion* of the Larmour circle.

DOI: 10.1103/PhysRevLett.100.086808 PACS numbers: 73.40.−c, 73.43.Qt, 78.67.−n

Introduction.—Originally, the cyclotron resonance (and its harmonics) in the ac conductivity, $\sigma(\omega)$, of the 2D electron gas had been detected by measuring the transmission of the microwave radiation [1]. In the recent experiment on high-mobility samples [2], it was demonstrated that this resonance, together with harmonics, also manifests itself in the dc magnetoresistance under microwave illumination, i.e., in the photoconductivity. The spectacular strength of this effect and, in particular, the observation of a zero-resistance state above a certain intensity of illumination [3–5], attracted the steady interest of researchers to the ac-response of a high-mobility electron gas in a weak magnetic field, B. Unlike the conventional Shubnikov–de Haas oscillations of the dc magnetoresistance, which vanish with temperature as $\exp(-2\pi^2 T/\omega_c)$, where ω_c is the cyclotron quantum, the magneto-oscillations of $\sigma(\omega)$ survive at high temperature [6,7]. The shape of these oscillations is given by [6,7]

$$\frac{\delta\sigma_{\pm}(\omega)}{\sigma_{\pm}(\omega)} = 2\cos\left(\frac{2\pi\omega}{\omega_c}\right)\exp\left(-\frac{2\pi}{\omega_c\tau}\right), \qquad (1)$$

where τ is the scattering time, and $\sigma_{\pm}(\omega)$ is related to the dc conductivity σ_0 as $\sigma_{\pm}(\omega) = \sigma_0/[2 + 2(\omega \pm \omega_c)^2\tau^2]$. Classically, the meaning of the damping factor $\delta^2 = \exp(-2\pi/\omega_c\tau) < 1$ is the probability for an electron to execute the entire Larmour circle, $2\pi R_L$, without being scattered. Oscillations Eq. (1) is a *single-electron* effect. In converting of these oscillations into the oscillating dc photoconductivity [7–10], the electron-electron interactions enter as a source of relaxation of the oscillatory part of the distribution function.

In the present paper we demonstrate that interactions *by themselves* give rise to the oscillatory contribution, $\delta\sigma^{\rm int}(\omega)$, to the *linear* ac conductivity, $\sigma(\omega)$, at frequencies much higher than in Eq. (1). To contrast this contribution to Eq. (1), we present $\delta\sigma^{\rm int}(\omega)$ in the form

$$\frac{\delta\sigma^{\rm int}(\omega)}{\sigma(\omega)} \propto \cos\left(C_\omega\frac{\omega}{\omega_c} - \frac{\pi}{4}\right)\exp\left[-\frac{3C_\omega}{\omega_c}\left(\frac{1}{\tau} + 2\pi T\right)\right], \qquad (2)$$

where

$$C_\omega = \left[\frac{32\omega}{27E_F}\right]^{1/2}, \qquad (3)$$

and E_F is the Fermi energy. Since C_ω is small, the correction Eq. (2) develops oscillations at much smaller magnetic fields $\omega_c \sim C_\omega\omega \ll \omega$ than Eq. (1). At such fields, the damping factor in Eq. (1) is $\sim\exp(-2\pi/C_\omega)$;, i.e., the conventional oscillations are completely washed out.

Qualitative picture.—The origin of the oscillations Eq. (2) lies in a peculiar modification by the interactions of the impurity scattering in a weak magnetic field. Conventionally [11–13], this modification amounts to the additional scattering [14] from the Friedel oscillations of the electron density, created by the impurity. Such a modification does not lead to the anomalous sensitivity to low B. However, as we demonstrate below, this sensitivity emerges in the *second order* in the electron-electron interaction strength. The corresponding second-order processes are illustrated in Figs. 1 and 2. The are the following. (i) A photoexcited electron emits a virtual pair, which is subsequently annihilated. Impurity scatters *not* the original electron, but rather the impurity scattering occurs between the states, *constituting the pair*, prior to annihilation. Diagram *b* in Fig. 2 describes this process. (ii) Electron is *not* scattered *directly* by the impurity, but rather experiences a *double* backscattering from the impurity-induced Friedel oscillations, as illustrated in Fig. 1, and also by the diagram *a* in Fig. 2.

We demonstrate that the corrections to the conductivity from both these processes *oscillate* with magnetic field according to Eq. (2). The oscillations reflect the fact that, for both processes, the dominant contribution to the double backscattering cross-section comes from two "distinguished" points that are located *symmetrically* with respect to the impurity at *certain* well-defined distance, $r_\omega \sim C_\omega R_L$, see Fig. 1. Then the argument of the cosine in Eq. (2) can be interpreted as a product ωt_ω, where

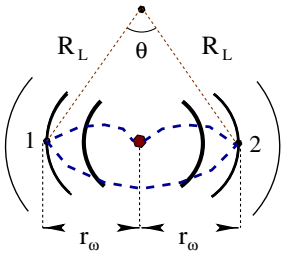

FIG. 1 (color online). Illustration of the B-dependent contribution, $\delta\Theta_B(r)$, to the phase of the polarization operator; $R_L[\theta - 2\sin(\theta/2)]$ is the elongation of the semiclassical trajectory due to the field-induced curving. The origin of oscillating magnetoconductivity is the scattering from the Friedel oscillations (arcs of decreasing thickness), at points 1 and 2, located *symmetrically* with respect to the impurity shown with a big dot.

$t_\omega = r_\omega/v_F$ is the time, during which the electron with Fermi velocity, v_F, travels the distance r_ω.

Derivation.—Although the interaction-induced oscillations come from small distances, $r_\omega \ll R_L$, we nevertheless will evaluate $\sigma(\omega)$ in the Landau gauge to demonstrate how both oscillations Eq. (1) and (2) emerge from the same calculation. Within the self-consistent Born approximation, averaging in the general expression for the diagonal conductivity

$$\sigma(\omega) = \frac{-e^2}{4\pi^3\Omega}\int_{-\infty}^{\infty}\frac{d\epsilon}{\omega}(f_\epsilon - f_{\epsilon+\omega})\mathrm{Tr}\overline{\hat{v}_x \mathrm{Im}\hat{G}_{\epsilon+\omega}\hat{v}_x \mathrm{Im}\hat{G}_\epsilon} \tag{4}$$

is decoupled into two averaged Green functions

$$G_\epsilon = \sum_n \overline{G_n(\epsilon)} = \sum_n \frac{1}{\epsilon - \epsilon_n - \Sigma_n(\epsilon)}, \tag{5}$$

where $\epsilon_n = (n + \frac{1}{2})\hbar\omega_c$ are the Landau levels, and $\Sigma_n(\epsilon)$ is the self-energy. In Eq. (4), the bar denotes the disorder averaging, Ω is the normalization area, and f_ϵ is the Fermi distribution. Upon decoupling, Eq. (4) takes a familiar form

$$\sigma_{\pm}(\omega) = \frac{e^2 v_F^2 \omega_c \nu_0}{8\pi}\int\frac{d\epsilon}{\omega}(f_\epsilon - f_{\epsilon+\omega}) \times \sum_n \mathrm{Im}G_{n\pm1}(\epsilon+\omega)\mathrm{Im}G_n(\epsilon), \tag{6}$$

where ν_0 is the 2D density of states. For high Landau levels, $(E_F/\hbar\omega_c) \gg 1$, in the first approximation in $\delta < 1$, the self-energy can be replaced by its zero-field value, $i/2\tau$. Then Eq. (6) readily reproduces the Drude conductivity. In order to capture the oscillatory ac magnetoconductivity, in the next approximation, one should take into account the "quantum" correction, $\delta\Sigma_n^Q(\epsilon) \propto \delta\exp(-2\pi i\epsilon/\omega_c)$, to the self-energy due to the discreteness of the Landau levels, as well as the interaction correction, $\delta\Sigma_n^{\mathrm{int}}(\epsilon)$. Since both corrections are smaller than $1/\tau$, they cause a small correction to the Green functions Eq. (5) of the form

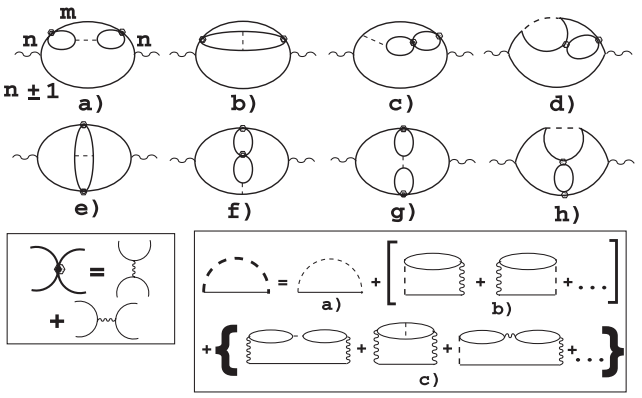

FIG. 2. Diagrams contributing to the second-order interaction correction to the ac magnetoconductivity. Dashed lines denote the impurity scattering. Dots in the vertices combine two types of the interaction matrix elements, as shown in the left inset. Diagrams b and e describe the impurity scattering of the *secondary* electron (hole); other diagrams describe double scattering of *photoexcited* electron (hole) by the Friedel oscillation. Right inset: diagram (a) for purely disorder-induced part of the self-energy, Σ_n, is plotted together with representative diagrams (b) and (c) for the interaction-induced self-energy, $\delta\Sigma_n^{int}$. Only diagrams (c), describing *two* electron-electron scattering processes, contribute to the interaction-induced magneto-oscillations.

$$\delta G_n(\epsilon) = \frac{\delta\Sigma_n^Q(\epsilon) + \delta\Sigma_n^{\mathrm{int}}}{(\epsilon - \epsilon_n - \frac{i}{2\tau})^2}. \tag{7}$$

The first and the second terms in Eq. (7) give rise to the oscillations Eq. (1) and Eq. (2), respectively. However, to reproduce these oscillations the quantum and the interaction corrections should be handled differently. To reproduce Eq. (1), upon substituting Eq. (7) into Eq. (6), one should keep the product, $\delta\Sigma_{n+1}^Q(\epsilon+\omega)[\delta\Sigma_n^Q(\epsilon)]^*$. It contains the oscillating term $\propto \exp(-2\pi i\omega/\omega_c)$, which *does not* depend neither on n nor on ϵ. For this reason, the resulting oscillations of magnetoconductivity are T independent. By contrast, to capture the interaction-induced oscillations, it is sufficient to keep $\delta\Sigma_n^{\mathrm{int}}$ only in one of the Green functions in Eq. (6), and its n-dependence is crucial. We will perform further calculation for $\delta\Sigma_n^{\mathrm{int}}(\epsilon)$ given by the first diagram of type c in Fig. 2 (inset). This is because the diagrams of type b do not cause magneto-oscillations, while the contributions of other diagrams of type c are comparable to that of the first one, and will be addressed later.

The first diagram of type c can be presented as

$$\delta\Sigma_n^{\mathrm{int}}(\epsilon) = \sum_m \frac{|R_{nm}|^2}{\epsilon - \epsilon_m + \frac{i}{2\tau}}, \tag{8}$$

so that the n dependence is encoded in the "matrix elements", R_{nm}. Substituting Eq. (8) into Eq. (7), and then Eq. (7) into Eq. (6) yields

$$\delta\sigma^{\rm int}(\omega) \propto \int \frac{d\epsilon}{\omega}(f_\epsilon - f_{\epsilon+\omega})\,{\rm Im}\sum_{n,m}\frac{|R_{nm}|^2}{(\epsilon - \epsilon_n + \frac{i}{2\tau})^2(\epsilon + \omega - \epsilon_{n\pm1} - \frac{i}{2\tau})(\epsilon - \epsilon_m + \frac{i}{2\tau})}. \quad (9)$$

As a next step, we express the matrix element, R_{nm}, as an integral in the coordinate space, following Fig. 2(c), $R_{nm} \propto \int d\mathbf{r}\psi_n^*(\mathbf{r})\psi_m(\mathbf{r})\Pi_0(\mathbf{r}, 0)$, where $\Pi_0(\mathbf{r}, 0)$ is the *static* polarization operator between the point $\mathbf{r} = 0$, where the impurity is located, and the point $\mathbf{r}$, where the backscattering takes place. Our prime observation is that with such R_{nm} the relevant term in Eq. (9), which has the form

$$-i\int d\epsilon(f_{\epsilon+\omega} - f_\epsilon)\frac{1}{\omega - \frac{i}{\tau}}\sum_{n,m}\frac{\psi_n^*(\mathbf{r}_1)\psi_n(\mathbf{r}_2)\psi_m^*(\mathbf{r}_2)\psi_m(\mathbf{r}_1)}{(\epsilon + \omega - \epsilon_{n\pm1} - \frac{i}{2\tau})(\epsilon - \epsilon_m + \frac{i}{2\tau})}, \quad (10)$$

again reduces to the polarization operator, $\Pi_{\omega\mp\omega_c}(\mathbf{r}_1, \mathbf{r}_2)$.

In the final expression for the interaction correction we make use of the fact that the B-dependence of this correction develops in the low-field limit $\omega_c \sim C_\omega\omega \ll \omega$, and replace $\omega \pm \omega_c$ by ω [15]. We then obtain

$$\frac{\delta\sigma^{\rm int}}{\sigma(\omega)} = \frac{\lambda^2}{\pi\nu_0^4\omega}\int d\mathbf{r}_1\int d\mathbf{r}_2 {\rm Im}\Pi_\omega(\mathbf{r}_1, \mathbf{r}_2){\rm Re}\{\Pi_0(0, \mathbf{r}_1)\Pi_0(\mathbf{r}_2, 0)\}, \quad (11)$$

where λ stands for dimensionless strength of interaction, which we assumed to be short-ranged. The numerical factor in Eq. (11) will be established when all the diagrams contributing to $\delta\sigma^{\rm int}$ are considered (see below).

Interpretation.—The form of Eq. (11) can be interpreted as follows. The factor, ${\rm Im}\Pi_\omega(\mathbf{r}_1, \mathbf{r}_2)$, in the integrand is the density-density response, the same as in calculation of the Drude ac conductivity. The second factor, ${\rm Re}\{\Pi_0(0, \mathbf{r}_1)\Pi_0(\mathbf{r}_2, 0)\}$, plays the role of the spatial correlator of the effective random potential. By lifting the momentum conservation, this potential enables the absorption of the ac field. If the correlator was $\propto \delta(\mathbf{r}_1 - \mathbf{r}_2)$, then the rhs of Eq. (11) would yield an ω-independent constant. Important is that the effective potential in Eq. (11) originates from the modulation of the electron density by the impurity, and thus *oscillates rapidly* with distance. It is these Friedel oscillations that in magnetic field lead to the oscillating correction, Eq. (2).

Oscillations.—The long-distance, $k_F r \gg 1$, behavior of the polarization operator in coordinate space is the following

$$\Pi_\omega(r) = -\frac{\pi\nu_0^2\hbar^4}{2k_F r}\left[i|\omega| + v_F\frac{\sin\{\Theta(r)\}}{r}A\left(\frac{2\pi rT}{v_F}\right)\right] \times \exp\left\{\frac{i|\omega|r}{v_F} - \frac{r}{v_F\tau}\right\}, \quad (12)$$

where the function $A(x) = x/\sinh(x)$ describes the temperature damping. In the momentum space, two contributions to Eq. (12) originate from small momentum transfer and momentum transfer close to $2k_F$, respectively [16]. At distances $r \ll R_L$, a nonquantizing magnetic field enters into Eq. (12) through the semiclassical phase, $\Theta(r)$. This phase is accumulated by the electron upon propagation from the point 0 to the point $\mathbf{r}$ *and back*. In a zero magnetic field, we obviously have, $\Theta(r) = 2k_F r$. At distances $r \ll R_L$, the field-dependent correction [17] to $\Theta(r)$ is equal to

$$\delta\Theta_B(r) = 2k_F\delta\mathcal{L} - \frac{\mathcal{A}B}{\Phi_0} = -\frac{E_F\omega_c^2 r^3}{6v_F^3}. \quad (13)$$

The origin of the correction Eq. (13) is illustrated in Fig. 1. It comes from elongation, $\delta\mathcal{L} = R_L[\theta - 2\sin(\theta/2)]$, of the classical electron trajectory in magnetic field, as well as from the Aharonov-Bohm flux into the *loop* with area $\mathcal{A} = (\theta - \sin\theta)R_L^2/2$. The correction Eq. (13) is *negative*, since the Aharonov-Bohm contribution *exceeds twice* the orbital contribution. We emphasize, that the conventional way [18] of incorporating magnetic field into the Green's function neglects the curvature of the electron trajectories, i.e., $\delta\Theta_B(r) = 0$. Thus, within the approach of Ref. [18], the oscillations Eq. (2) *would not* emerge.

Further calculation is straightforward. Substituting Eq. (12) into Eq. (11), performing the angular integration, and combining rapidly oscillating terms in the product of three polarization operators into a "slow" term, we find that the interaction correction Eq. (11) can be presented as $\delta\sigma^{\rm int}/\sigma(\omega) = (\lambda^2 E_F/\omega)F_{\tau,T}$, where the dimensionless function $F_{\tau,T}(\omega, \omega_c)$ is defined as follows

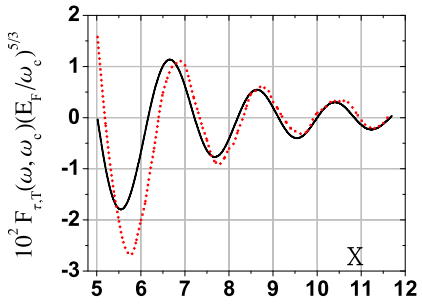

FIG. 3 (color online). Interaction-induced contribution to the ac conductivity calculated numerically from Eq. (14) (dotted line) and from asymptotic expression Eq. (16) (full line) are plotted vs dimensionless frequency $x = 2^{1/3}\omega/(E_F^{1/3}\omega_c^{2/3}) = 3(z/4)^{2/3}$. The calculations are performed for dimensionless disorder $1/(E_F\tau) = 0.08(\omega_c/E_F)^{2/3}$ and dimensionless temperature $T/E_F = 0.06(\omega_c/E_F)^{2/3}$.

$$F_{\tau,T} = \frac{1}{(\pi k_F)^{5/2}} \int_0^\infty \frac{dr_1 dr_2}{[r_1 r_2 (r_1 + r_2)]^{3/2}} A\left(\frac{2\pi r_1 T}{v_F}\right) A\left(\frac{2\pi r_2 T}{v_F}\right) A\left(\frac{2\pi (r_1 + r_2) T}{v_F}\right) \exp\left\{-\frac{2(r_1 + r_2)}{v_F \tau}\right\} \times \cos\left[\frac{\omega (r_1 + r_2)}{v_F} + \delta\Theta_B(r_1 + r_2) - \delta\Theta_B(r_1) - \delta\Theta_B(r_2) - \frac{\pi}{4}\right]. \quad (14)$$

Other slow terms emerging in the rhs of Eq. (11), e.g., the one with $\omega \to -\omega$, do not oscillate with magnetic field. By contrast, the function $F_{\tau,T}$ *does* oscillate, since the argument of cosine in Eq. (14), with $\delta\Theta_B$ given by Eq. (13), has a *saddle point* at $r_1 = r_2 = r_\omega = 3C_\omega v_F/4\omega_c = (3/4)C_\omega R_L$. In the vicinity of the saddle point, the phase of the cosine can be presented as

$$\frac{C_\omega \omega}{\omega_c} - \frac{\pi}{4} - \frac{C_\omega \omega}{\omega_c}\left[\frac{(r_1 - r_\omega)^2 + (r_2 - r_\omega)^2}{4r_\omega^2} + \frac{(r_1 - r_\omega)(r_2 - r_\omega)}{r_\omega^2}\right], \quad (15)$$

where C_ω is defined by Eq. (2). Note, that the combination, $[C_\omega \omega/\omega_c - \frac{\pi}{4}]$, in (15) is nothing but the phase of the interaction-induced oscillations Eq. (2). It also follows from Eq. (15) that, when this phase is large, the characteristic deviations, $(r_1 - r_\omega)$ and $(r_2 - r_\omega)$ are much smaller than r_ω. This allows us to perform the integration over these deviations in Eq. (14) *explicitly*. This yields

$$F_{\tau,T}(\omega, \omega_c) = \frac{1}{(3 \times 2^{29/3}\pi^3)^{1/2}} \left(\frac{\omega_c}{E_F}\right)^{5/3} D\left(\frac{C_\omega \omega}{\omega_c}\right) \cos\left(\frac{C_\omega \omega}{\omega_c} - \frac{\pi}{4}\right) A^2\left(\frac{2\pi r_\omega T}{v_F}\right) A\left(\frac{4\pi r_\omega T}{v_F}\right) \exp\left[-\frac{4r_\omega}{v_F \tau}\right], \quad (16)$$

where $D(z) = z^{-5/6}$. For high enough temperatures $T > 2\omega_c/3\pi C_\omega$ (but still $T \ll \omega$), the damping factor can be replaced by the exponent, and we reproduce the oscillating contribution Eq. (2). The above derivation suggests that oscillatory behavior of the correction Eq. (2) establishes only at large $z \gg 1$, which corresponds to the nodes of $\cos(z - \pi/4)$ with high numbers. To find out where the asymptotics Eq. (16) actually applies, we have evaluated the double integral Eq. (14) numerically. The result is plotted in Fig. 3 and indicates that Eq. (2) applies starting already from the third node.

Other diagrams.—Contribution Eq. (16) to $\delta\sigma^{\text{int}}(\omega)$ is the result of calculation of a single diagram *a* in Fig. 2. Other diagrams, involving two electron-electron scattering processes and yielding contributions with a structure similar to Eq. (16), are shown in Fig. 2. Diagrams *b*, *c*, and *d* are captured within the self-consistent Born approximation, and correspond to certain terms in $\delta\Sigma^{\text{int}}$, see (c) in Fig. 2 (inset). Diagrams $e - h$ in Fig. 2 are of the same order as $a - d$, but they are *not* contained in Eq. (6); these diagrams emerge from the general expression Eq. (4) for $\sigma(\omega)$. Taking all the diagrams into account leads to the modification of the function $D(z)$ from $z^{-5/6}$ to $\tilde{D}(z) = -32z^{-5/6} + 64z^{1/6}$, where the factors -32 and 64 account for the spin indices and for the number of closed fermion loops in different diagrams. The second term, $\propto z^{1/6}$, arises from the diagrams *b*, *e* and *d*, *h* in Fig. 2. Since the oscillations in Eq. (2) develop at $z \gg 1$, these diagrams are, actually, dominant.

Numerical estimates.—Note that, in terms of *B* periodicity, oscillations Eq. (2) coincide with oscillations Eq. (1) upon rescaling ω_c by $2\pi/C_\omega$ in the argument of cosine, and by $2\pi/3C_\omega$ in the Dingle factor. For a typical ac frequency $\hbar\omega \sim 3$ K and density $n \sim 10^{11}$ cm^{-2} in the experiments [2–5,19,20] this shifts the domain of oscillations Eq. (2) from $B \sim 0.2$ T to $B \lesssim 10^{-2}$ T. For such *B* the observation of the oscillations requires $T < \omega_c/6\pi C_\omega \sim 20$ mK, which was not the case in Refs. [2–5,19,20]. For observation of magneto-oscillations Eq. (2) higher densities $n \sim 5 \times 10^{11}$ cm^{-2} and frequencies $\hbar\omega \sim 15$ K are needed.

[1] J. P. Kotthaus, G. Abstreiter, and J. F. Koch, Solid State Commun. **15**, 517 (1974).
[2] M. A. Zudov *et al.*, Phys. Rev. B **64**, 201311 (2001).
[3] M. A. Zudov *et al.*, Phys. Rev. Lett. **90**, 046807 (2003).
[4] R. G. Mani *et al.*, Nature (London) **420**, 646 (2002).
[5] S. I. Dorozhkin, JETP Lett. **77**, 577 (2003).
[6] I. A. Dmitriev, A. D. Mirlin, and D. G. Polyakov, Phys. Rev. Lett. **91**, 226802 (2003).
[7] I. A. Dmitriev, A. D. Mirlin, and D. G. Polyakov, Phys. Rev. B **70**, 165305 (2004).
[8] M. G. Vavilov and I. L. Aleiner, Phys. Rev. B **69**, 035303 (2004).
[9] I. A. Dmitriev *et al.*, Phys. Rev. B **71**, 115316 (2005).
[10] I. A. Dmitriev, A. D. Mirlin, and D. G. Polyakov, Phys. Rev. B **75**, 245320 (2007).
[11] A. Gold and V. T. Dolgopolov, Phys. Rev. B **33**, 1076 (1986).
[12] G. Zala, B. N. Narozhny, and I. L. Aleiner, Phys. Rev. B **64**, 214204 (2001).
[13] I. V. Gornyi and A. D. Mirlin, Phys. Rev. B **69**, 045313 (2004).
[14] A. M. Rudin, I. L. Aleiner, and L. I. Glazman, Phys. Rev. B **55**, 9322 (1997).
[15] For the same reason we neglect the Zeeman splitting.
[16] A. V. Chubukov and D. L. Maslov, Phys. Rev. B **68**, 155113 (2003); **69**, 121102 (2004).
[17] T. A. Sedrakyan, E. G. Mishchenko, and M. E. Raikh, Phys. Rev. Lett. **99**, 036401 (2007).
[18] L. P. Gor'kov, Zh. Eksp. Teor. Fiz. **36**, 1918 (1959).
[19] S. A. Studenikin *et al.*, Solid State Commun. **129**, 341 (2004).
[20] A. A. Bykov *et al.*, arXiv:cond-mat/0603398.